JOURNAL OF SOLID STATE CHEMISTRY 37, 302–307 (1981)

Phase Transitions in CsH_2AsO_4 at High Pressures and Temperatures

S. HART, P. W. RICHTER, AND J. B. CLARK

National Physical Research Laboratory, Council for Scientific and Industrial Research, P.O. Box 395, Pretoria 0001, South Africa

AND E. RAPOPORT

Soreq Nuclear Research Centre, Yavne, Israel

Received July 24, 1980; in final form September 16, 1980

CsH_2AsO_4 (CDA) is an analog of the well-known ferroelectric KH_2PO_4 (KDP). The phase diagram of CDA has been established to the melting curve and up to 4 GPa. Evidence for three new phases has been found.

Introduction

The ferroelectric materials of the KDP (KH_2PO_4) family have been studied extensively over the years, particularly in the region of the ferroelectric–paraelectric phase transition, which is typically well below ambient temperature. In a continuing effort, materials of this family are being investigated in the high-temperature–high-pressure regime and the results for CDA (CsH_2AsO_4) to 4 GPa and 400°C are reported here.

The ferroelectric phase is orthorhombic (space group *Fdd*2) and transforms to a tetragonal paraelectric phase ($I\bar{4}2d$) at a temperature of 139 K (*1*). The ferroelectric properties of this material were first reported in 1953 (*2*) and high-temperature transitions have been reported (*3*). In a DTA (differential thermal analysis) study on deuterated CDA, Loiacono *et al.* (*1*) noted that some DTA signals died out on cycling until only one stable signal was left. It was suggested that a single phase transition with slow kinetics was the cause of this behavior and it may be that some of the reported transitions for CDA are spurious. In the higher temperature region the decomposition of CDA with the loss of water is another problem which may complicate the interpretation of apparent phase behavior.

Experimental

CDA was prepared from arsenic acid and caesium carbonate following the procedure of Shklovskaya and Arkhipov (*4*). The X-ray diffraction data characterized the material well. To investigate possible decomposition at elevated temperatures, some CDA was cycled to 400°C in an open boat. The X-ray pattern obtained for the material back at room temperature again, although tending to show some extra lines, was still dominantly that of CDA.

Gallagher (*5*) in thermogravimetric experiments has shown that although the 0.1% weight loss temperature is 149°C, the

0022-4596/81/060302-06$02.00/0

main feature for CDA is the very sharp loss of weight at 300°C associated with the decomposition.

Differential scanning calorimetry (DSC) experiments were carried out in sealed containers using a DuPont Thermal Analyzer Model 990. Evidence for two-phase transitions was seen at 123 and 165°C before variable nonrepeatable signals, probably indicating the onset of decomposition, were obtained. The lower temperature signal was obtained on the first run up in temperature and was repeatable both on cooling and heating provided the temperature was not taken above the second transition. If this happened, the 123°C transition signal was only recovered after some hours of relaxation at ambient temperature. The 165°C transition, however, was repeatable anytime provided the decomposition region above 200°C was not entered. Transition enthalpies of 0.52 and 7.83 kJ $mole^{-1}$ were obtained for the 123 and the 165°C transitions, respectively. DSC signals of a typical first run up in temperature are shown in Fig. 1.

The high-pressure techniques using a piston–cylinder apparatus and differential thermal analysis have been fully described in other publications from this laboratory (e.g., Pistorius and Clark (*6*), Richter and Pistorius (*7*)).

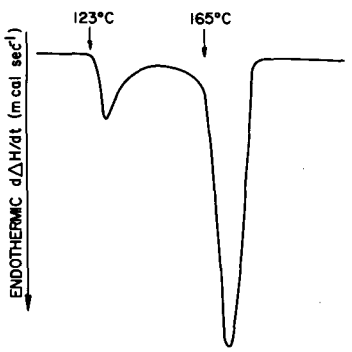

FIG. 1. Differential scanning calorimetry signals for CDA.

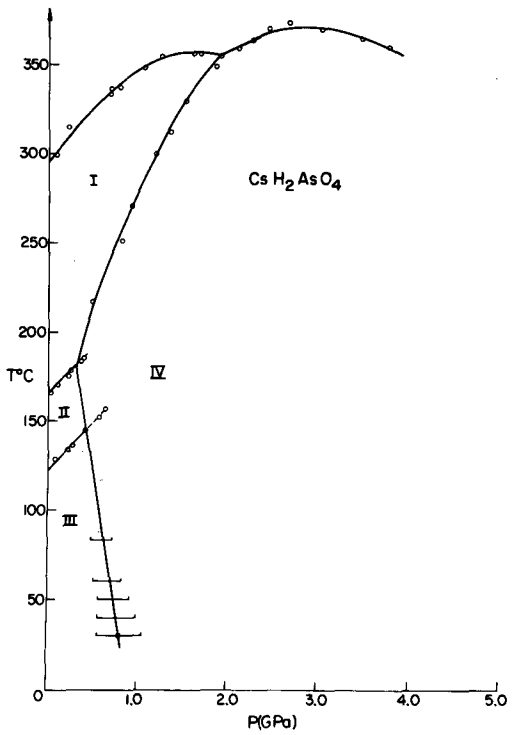

FIG. 2. Phase diagram of CDA.

The samples were contained in niobium capsules and showed no signs of decomposition or contamination when examined by X-ray diffraction after the pressure runs. Chromel–alumel thermocouples were used and corrections for the effect of pressure on thermal emf (*8*) and for symmetric and asymmetric friction (*9*) were applied to the raw data. To investigate a sluggish transition near ambient temperature, the volumetric technique described by Clark (*10*) was followed.

Results

The phase diagram for CDA is shown in Fig. 2. The boundary between phases III and II was followed not allowing the temperature to overshoot by more than 10°C since, in common with the DSC signals described above, the DTA signal was lost if

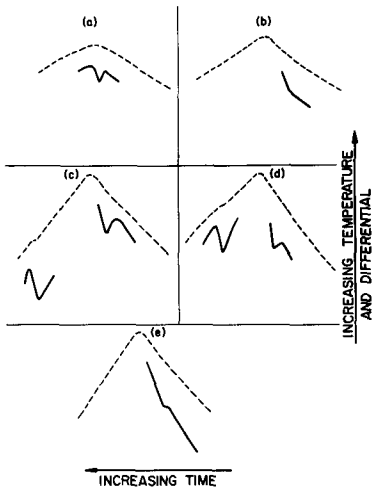

FIG. 3. Typical DTA signals for CDA. (a) II/III boundary, (b) I/II boundary, (c) I/IV boundary, (d) I/Liquid boundary, (e) IV/Liquid boundary.

the 165°C higher transition was crossed during the run. Above a pressure of about 0.6 GPa the signal quality degraded until no signal was seen at all around 0.8 GPa. The I/II boundary was easily followed but no signal quality deteriorated above 0.4 GPa. Examples of signals are shown in Figs. 3a and b. It is believed that the poor-quality signal parts of these boundaries are on metastable extensions of the true phase boundaries.

In general in this work on CDA the cooling DTA signals were smaller, more diffuse and depressed in temperature by 10 to 30°C compared with the heating signals. Only heating signal data have been used. The estimated accuracy is ±0.05 GPa and ±2°C unless otherwise indicated.

A boundary breaks away from the I/II phase line and rises very sharply to intersect the melting curve at about 2 GPa. Examples of signals on these boundaries are also given in Fig. 3. This melting curve was followed down in pressure and the atmospheric melting temperature is estimated to be 295°C. The fitted curve shows a flattish maximum at 1.63 GPa and 358°C but this is thought to be more a consequence of the distribution of the data points in the least-squares analysis and it is not claimed that this maximum has physical significance. However, above the triple point there is a pronounced maximum which was experimentally observed.

A search for DTA signals in the low pressure and temperature region near the observed I/II and II/III boundaries proved futile, indicating the possible existence of a large volume change transition. However, the volumetric technique proved fruitful and clear results were obtained indicating a triple point at 0.4 GPa and 145°C. The piston displacement results for the volumetric work at 49°C are shown in Fig. 4 for upstroke and downstroke, indicating a transition on the pressure range 0.5–0.9 GPa. With the known initial volume of the sample, the average volume change for the transitions measured on this III/IV boundary is 3.5%. Following the procedure suggested by Wolbarst *et al.* (*11*), the new

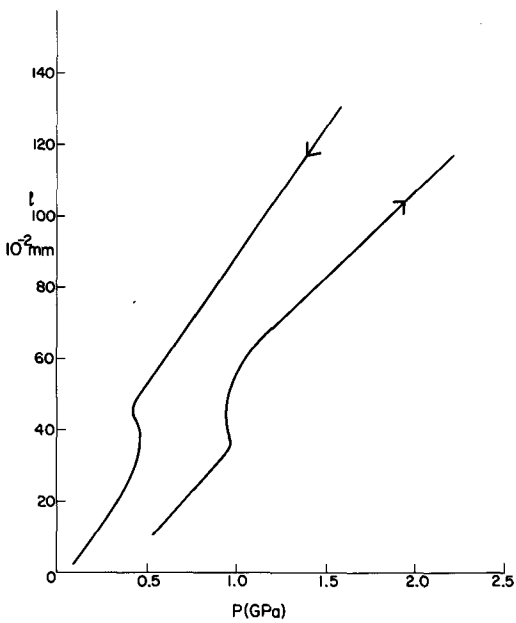

FIG. 4. Volumetric results–upstroke and downstroke.

boundary is shown in Fig. 2 with error bars indicating the region of indifference of the transition.

Since data on the II/IV boundary were not obtained and data near the start of the I/IV boundary were sparse, the following procedure was followed. The entropy at 123°C and ambient pressure was assumed constant for the II/III phase line and using the Clausius–Clapeyron equation this gave a value of 6.5 10^{-8} m^3 $mole^{-1}$ for ΔV. For the III/IV boundary both ΔV and dP/dT were known so that dP/dT for the II/IV boundary could be obtained from the general relation for a triple point

$$\left(\frac{dP}{dT}\right)_{13}(\Delta V_{12} + \Delta V_{23}) = \left(\frac{dP}{dT}\right)_{12}\Delta V_{12} + \left(\frac{dP}{dT}\right)_{23}\Delta V_{23}.$$

This relationship follows from the two facts that at a 1/2/3 triple point

$$\Delta V_{13} = \Delta V_{12} + \Delta V_{23},$$

and

$$\Delta H_{13} = \Delta H_{12} + \Delta H_{23} \qquad (H = \text{enthaply}).$$

The II/IV boundary which was then assumed linear intersected the I/II line to give the I/II/IV triple point. The same procedure around this triple point then gave the initial slope of the I/IV phase line. This was found to be in good agreement with the least-squares fit to the data, which is given in Table I. The triple-point coordinates are given in Table II.

TABLE I

PHASE RELATIONS

Boundary	Least-squares fit[a]
III/II	$t = 123 + 53.4P$
II/I	$t = 165 + 54.0P$
I/Liquid	$t = 296 + 75.6P - 23.1P^2$
III/IV	$t = 270 - 303.0P$
II/IV	$t = 287 - 345.0P$
I/IV	$t = 182 + 169.4(P - 0.3) - 38.9(P - 0.3)^2$
IV/Liquid	$t = 355 + 34.9(P - 1.9) - 18.2(P - 1.9)^2$

[a] t in °C, P in GPa.

TABLE II

COORDINATES OF TRIPLE POINTS

Triple point	P (GPa)	t (°C)
III/II/IV	0.41	145
II/I/IV	0.30	182
I/IV/Liquid	1.92	355

Discussion

The phase diagram of CDA should be considered in relation to other members of the KDP family. A complete clear pattern does not exist for the family's phase behavior, although some common features emerge. The general trend on increasing temperature at ambient pressure is to progress from the ferroelectric orthorhombic structure to the tetragonal and then to the less symmetric monoclinic structure. However, a notable exception to this is CDP where the orthorhombic structure changes to monoclinic directly. Other high-temperature phases of unknown structure have been found during high-pressure work where it has commonly been found that a little pressure will stabilize these materials and stop the decomposition by loss of water (e.g., (*12*)). Considerable uncertainty exists also for the precise phase transition temperatures. Thus Grunberg *et al.* (*13*) suggest two transitions for KDP at 130 and 175°C and two for RDP at 86 and 175°C from their measurements on dielectric constants and infrared reflection. On the other hand, Rapoport (*14*) using differential thermal analysis on KDP reported transitions at 190 and 233°C. It was assumed that the 175 and 190°C transitions were the same but the questions remain as to which phase is monoclinic and what the nature of the other phases might be. The same problem applies

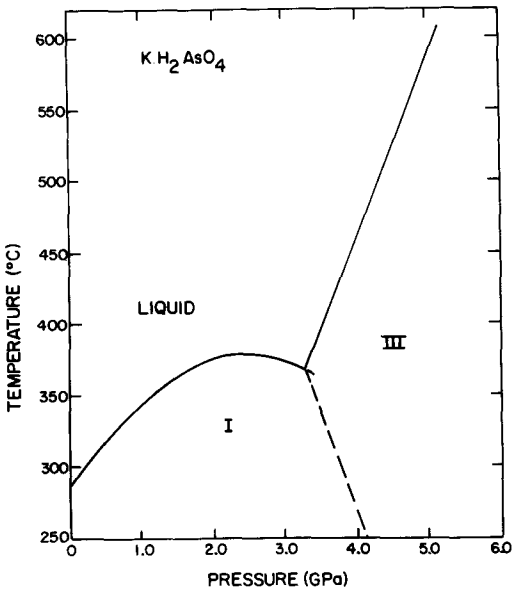

FIG. 5. Phase diagram for KDA (*10*).

to RDP where Rapoport *et al.* (*12*) reported transitions at 90 and 281°C.

Only one paper for high-pressure–high temperature phase diagrams of the arsenate

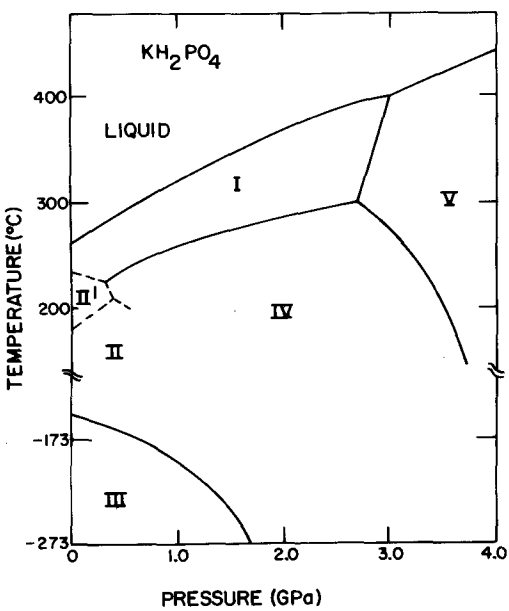

FIG. 6. Phase diagram for KDP (*14*).

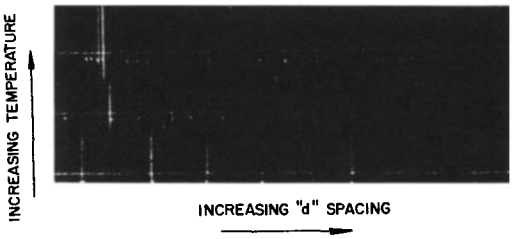

FIG. 7. High-temperature powder patterns for CDA.

analogs of the KDP family exist, that of Clark (*10*) for KDA. The diagram (Fig. 5) is much more simple than that for KDP, with the tetragonal room temperature phase being stable to the melting curve at low pressure and only one high-temperature phase being seen above 350°C and 3.5 GPa. This simplification is not seen for CDA where the diagram is similar to that for CDP (*12*), but there can be no 1:1 correspondence of phases since the room temperature phase of CDP is monoclinic, and not tetragonal as mentioned above. Similarity of the diagrams for CDA and KDP (Fig. 6) is also superficially evident where in addition the existence of the quasi-irreversible transition to phase II′ seems consistent.

High-temperature X-ray powder patterns taken at 140 and 180°C for CDA (Fig. 7) show the existence of the two new crystal phases but these have not been indexed and full crystal structure data for the other family members do not, as yet, exist. Attempts to quench out the high-pressure phase IV were unsuccessful. Loiacono (*1*) reported a monoclinic unit cell for 85% deuterated CDA (DCDA) at temperatures above 170°C. Since the ambient condition unit cells for CDA and DCDA are almost identical, it is almost tempting to assume one of the high-temperature CDA phases would be very similar to that observed for DCDA. However, the X-ray patterns do not resemble one another. In this regard though, it is worth remembering that deuteration can change radically the physical properties of these materials. Kennedy *et*

al. (*15*) have shown that a monoclinic room temperature KDP phase can be made stable on suitable deuteration and this will not change to the tetragonal or to the orthorhombic structure down to 6 K.

It would obviously be of great value to have the crystal structures of the high-temperature phases of these materials determined.

Acknowledgments

The authors are very grateful to M. Thomas for his D.S.C. work, to A. I. Kingon for valuable discussions and to J. J. Erasmus and his staff for the upkeep of the apparatus and for the manufacture of components. The calculations were done on the CDC 174 computer of the Centre for Computing Services.

References

1. G. M. Loiacono, J. Ladell, W. N. Osborne and J. Nicolosi, *Ferroelectrics* **14,** 761 (1976).
2. B. C. Frazer and R. Pepinsky, *Phys. Rev.* **91,** 212 (1953).
3. J. Y. Nicholson, III, and J. F. Soest, *J. Chem. Phys.* **60,** 715 (1974).
4. R. M. Shklovskaya and S. M. Arkhipov, *Russian J. Inorg. Chem.* **12,** 1234 (1967).
5. P. K. Gallagher, *Thermochim. Acta* **14,** 131 (1976).
6. C. W. F. T. Pistorius and J. B. Clark, *High Temp. High Press.* **1,** 561 (1969).
7. P. W. Richter and C. W. F. T. Pistorius, *J. Solid State Chem.* **3,** 197 (1971).
8. R. E. Hanneman and H. M. Strong, *J. Appl. Phys.* **37,** 614 (1966).
9. C. W. F. T. Pistorius, E. Rapoport, and J. B. Clark, *Rev. Sci. Instrum.* **38,** 1741 (1967).
10. J. B. Clark, *High Temp. High Press.* **1,** 553 (1969).
11. A. B. Wolbarst, J. B. Clark, and P. W. Richter, *Rev. Sci. Instrum.* **49,** 11 (1978).
12. E. Rapoport, J. B. Clark, and P. W. Richter, *J. Solid State Chem.* **24,** 423 (1978).
13. J. Grunberg, S. Levin, I. Pelah, and D. Gerlich, *Phys. Stat. Sol.* (b) **49,** 857 (1972).
14. E. Rapoport, *J. Chem. Phys.* **53,** 311 (1970).
15. N. S. J. Kennedy, R. J. Welmes, F. R. Thornley, and K. D. Rouse, *Ferroelectrics* **14,** 591 (1976).